RAPID COMMUNICATIONS

PHYSICAL REVIEW B **89**, 020504(R) (2014)

Superconducting proximity effect in silicene: Spin-valley-polarized Andreev reflection, nonlocal transport, and supercurrent

Jacob Linder[1] and Takehito Yokoyama[2]

[1]*Department of Physics, Norwegian University of Science and Technology, N-7491 Trondheim, Norway*

[2]*Department of Physics, Tokyo Institute of Technology, Tokyo 152-8551, Japan*

(Received 31 July 2013; revised manuscript received 24 December 2013; published 10 January 2014)

We theoretically study the superconducting proximity effect in silicene, which features massive Dirac fermions with a tunable mass (band gap), and compute the conductance across a normal-superconductor (N-S) silicene junction, the nonlocal conductance of an N-S-N junction, and the supercurrent flowing in an S-N-S junction. It is demonstrated that the transport processes consisting of local and nonlocal Andreev reflection may be efficiently controlled via an external electric field owing to the buckled structure of silicene. In particular, we demonstrate that it is possible to obtain a fully spin-valley-polarized crossed Andreev reflection process without any contamination of elastic cotunneling or local Andreev reflection, in stark contrast to ordinary metals. It is also shown that the supercurrent flowing in the S-N-S junction can be fully spin-valley polarized and that it is controllable by an external electric field.

DOI: 10.1103/PhysRevB.89.020504 PACS number(s): 73.23.−b

With the advent of graphene [1] and topological insulators [2], the study of Dirac fermions in condensed matter systems [3] has become one of the most active research fields in physics over the past decade. Condensed matter systems with such a "relativistic" electronic band structure are intriguing examples of low-energy emergent symmetries (in this case, Lorentz invariance). This has led to a tremendous amount of interest in terms of possible application value as well as from a fundamental physics viewpoint.

One of the most recent advances in this field has been the synthesis of silicene [4] which consists of silicon atoms arranged in a honeycomb pattern with a buckled sublattice structure [5]. As in graphene, the states near the Fermi energy may be described by Dirac theory at two valleys K and K', but an important difference is that the fermions are massive in silicene due to a spin-orbit coupling which is much larger than in graphene. As a result, silicene is under the right circumstances a quantum spin Hall insulator with topologically protected edge states. In fact, it is possible [6] to achieve a rich variety of topological states in silicene due to a unique feature: The buckled structure causes the sublattices to respond differently to an applied electric field, which in turn induces a fermion mass gap which is tunable. Closing and reopening this gap allows for a transition between different topological phases at a critical field value $|E_z| = E_c$, as shown in Fig. 1(a).

The combination of a superconducting proximity effect with topologically protected edge states is currently generating a lot of interest due to the possibility of creating Majorana fermions in this manner [2,7–10]. However, studies of proximity-induced superconductivity in silicene are still lacking. In this Rapid Communication, we investigate precisely this topic and focus on the signature of the Andreev reflection process, both locally and nonlocally [which is usually dubbed crossed Andreev reflection (CAR)]. We find that the possibility to tune both the band gap via an electric field E_z as well as the local Fermi level via a gate voltage provides an unparalleled control over the Andreev reflection process in silicene. In particular, we find that it is possible to generate a pure crossed Andreev reflection signal without any contamination from elastic cotunneling. It is also shown that the supercurrent flowing in the superconductor-normal-superconductor (S-N-S) junction may be fully spin-valley polarized and that it is controllable by an external electric field. This finding, combined with the observation that the Andreev reflection process is fully spin-valley polarized, as will be described in detail later, demonstrates that silicene provides a unique environment for obtaining controllable superconducting transport with no counterpart in graphene or topological insulators. These results may pave the way for different perspectives for quantum transport polarized with different degrees of freedom, namely, the combined spin-valley product.

We consider a silicene layer made up by a buckled honeycomb lattice consisting of two sublattices A and B [11]. Using a tight-binding formalism, one obtains the following lattice Hamiltonian [6,12,13]:

$$\begin{aligned} H = &-t \sum_{\langle i,j\rangle,\alpha} c_{i\alpha}^\dagger c_{j\alpha} + \frac{i\lambda}{3\sqrt{3}} \sum_{\langle\langle i,j\rangle\rangle,\alpha,\beta} \nu_{ij} c_{i\alpha}^\dagger \sigma_{\alpha\beta}^z c_{j\beta} \\ &+ l \sum_{i\alpha} \zeta_i E_z^i c_{i\alpha}^\dagger c_{i\alpha} - \mu \sum_{i\sigma} c_{i\sigma}^\dagger c_{i\sigma} \\ &+ \sum_{i\sigma} (\sigma \Delta_0 c_{i\sigma}^\dagger c_{i,-\sigma}^\dagger + \text{H.c.}). \end{aligned} \quad (1)$$

Here, t is the hopping element, λ is the effective spin-orbit coupling parameter, $2l$ is the separation between the A and B sublattices in the z direction, E_z is an applied electric field, $\zeta_i = \pm 1$ for the A (B) sites is the staggered sublattice potential term, while $\nu_{ij} = (\mathbf{d}_i \times \mathbf{d}_j)/|\mathbf{d}_i \times \mathbf{d}_j|$ having defined $\mathbf{d}_i$ and $\mathbf{d}_j$ as the two nearest bonds connecting the next-nearest neighbors. To describe quantum transport in the presence of a superconducting proximity effect, we derive an effective low-energy theory [11] for excitations near the Dirac points K_η, $\eta = \pm$. In the end, we obtain the following $\mathbf{k}$-space Hamiltonian when using a basis

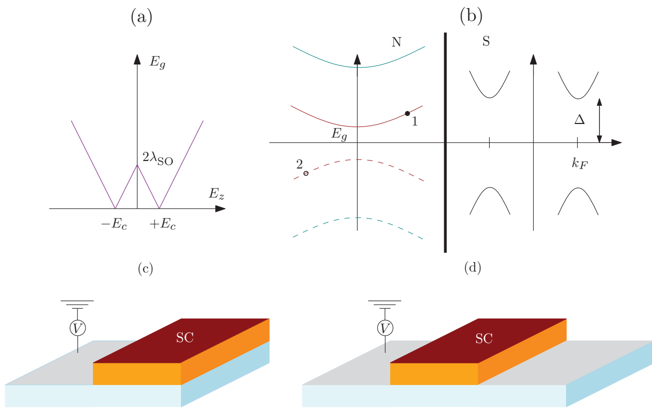

FIG. 1. (Color online) (a) Plot of the insulating gap E_g of normal-state silicene vs an applied electric field E_z perpendicular to the plane. (b) Band structure in an N-S silicene junction. The two conduction bands are split at $\mathbf{k} = 0$. The process "1" indicates an incoming quasiparticle from one of the conduction bands, whereas "2" indicates the lost electron in the valence band when Andreev reflection occurs. (c) An effective N-S silicene bilayer where superconductivity is induced via a proximate superconducting lead. (d) An effective N-S-N silicene junction to probe nonlocal transport.

$$\psi_{\mathbf{k}}^\dagger = [(\psi_{\mathbf{k},\sigma}^A)^\dagger,(\psi_{\mathbf{k},\sigma}^B)^\dagger,\psi_{-\mathbf{k},-\sigma}^A,\psi_{-\mathbf{k},-\sigma}^B]:$$

$$H_{\sigma,\mathbf{K}_\eta+\mathbf{k}} = \psi_{\mathbf{k}}^\dagger H_{\eta,\sigma}(\mathbf{k})\psi_{\mathbf{k}},\ H_{\eta,\sigma}(\mathbf{k}) = \begin{pmatrix} \hat{H}_0 & \sigma\Delta_0\hat{1} \\ \sigma\Delta_0^\dagger\hat{1} & -\hat{H}_0 \end{pmatrix},$$
$$\hat{H}_0 = (lE_z - \eta\sigma\lambda_{SO})\hat{\tau}_z - \mu\hat{1} + v_F(\eta k_x\hat{\tau}_x - k_y\hat{\tau}_y), \tag{2}$$

with $\lambda_{SO} = \lambda/2$. Since we shall consider a hybrid junction consisting of normal silicene and a silicene region with proximity-induced superconductivity, it is instructive to discuss the eigenvalues and band structure in these regions separately. In the normal state, silicene is an insulator with topological properties that may be controlled by an external electric field, as discussed previously. The excitation energies read $E_{\eta,\sigma}(\mathbf{k}) = \pm\sqrt{k^2 + (lE_z - \eta\sigma\lambda_{SO})^2}$, having set the chemical potential $\mu_N = 0$. The gap between the conduction and valence band is then $E_g = 2|lE_z - \eta\sigma\lambda_{SO}|$ and we set $v_F = 1$ for brevity of notation.

To allow for proximity-induced superconductivity in the region $x > 0$, it is natural to include an electric doping level and thus a chemical potential $\mu_S \gg \lambda_{SO},\Delta_0$ in order to have a finite carrier density at the Fermi level. The eigenvalues then read $E_{\eta,\sigma}(\mathbf{k}) = \pm\sqrt{[\sqrt{k^2 + (lE_z - \eta\sigma\lambda_{SO})^2} \pm \mu_S]^2 + |\Delta_0|^2}$. It is now instructive to compare the band structures in the N and S regions visually, as done in Fig. 1(b). It is seen that in order for Andreev reflection to occur, the excitation gap in the N part must be smaller than the proximity-induced superconducting gap Δ_0. In this way, an incoming electronlike quasiparticle from the N side with energy E (which must satisfy $E > E_g/2$ since there exist no states within the insulating gap) may be either normally reflected within the same conduction band or Andreev reflected. In the latter case, an electron of opposite spin is removed from the valence band and consequently the Andreev reflection process in undoped silicene is intrinsically *specular*: The Andreev-reflected hole has a group velocity parallel to its momentum.

Based on these observations, we are now in a position to write down the wave functions in the N and S regions as follows. At the interface $x = 0$, we find that

$$\begin{aligned}\psi_N &= \frac{1}{\sqrt{2E\tau_+}}[\eta k_F e^{i\eta\theta},\tau_+,0,0] \\ &\quad + \frac{r_e}{\sqrt{2E\tau_+}}[-\eta k_F e^{-i\eta\theta},\tau_+,0,0] \\ &\quad + \frac{r_h}{\sqrt{2E\tau_-}}[0,0,\eta k_F e^{-i\eta\theta},\tau_-], \\ \psi_S &= \frac{t_e}{\sqrt{2}}[\eta e^{i\eta\theta_S}u_+,u_+,\eta e^{i\eta\theta_S}u_- e^{-i\phi},u_- e^{-i\phi}] \\ &\quad + \frac{t_h}{\sqrt{2}}[-\eta e^{-i\eta\theta_S}u_- e^{i\phi},u_- e^{i\phi},-\eta e^{-i\eta\theta_S}u_+,u_+].\end{aligned} \tag{3}$$

The scattering coefficients $r_{\eta,\sigma}^e$, $r_{\eta,\sigma}^h$, $t_{\eta,\sigma}^e$, $t_{\eta,\sigma}^h$ denote normal reflection, Andreev reflection, and transmission as electronlike and holelike quasiparticles, respectively. The angle of incidence and transmission are related via $k_F\sin\theta = \mu\sin\theta_S$, where $k_F = \sqrt{E^2 - (lE_z - \eta\sigma\lambda_{SO})^2}$ and we have defined $\tau_\pm = E \pm (\eta\sigma\lambda_{SO} - lE_z)$ in addition to $u_\pm = [1/2 \pm \sqrt{E^2 - \Delta_0^2}/2E]^{1/2}$. We note in passing that since the incident quasiparticles must have $E > (\eta\sigma\lambda_{SO} - lE_z)$ in order to exceed the insulating gap, $\tau_\pm$ is always real and positive. Since $\mu_S \gg k_F$, we may set $\theta_S = 0$ for more transparent results.

The scattering coefficients may now be computed by matching the wave functions at the interface $x = 0$ (as follows from conservation of current flux, $\hat{v}_x\psi$ with $\hat{v}_x = \partial\hat{H}/\partial k_x$) and subsequently used to find the conductance spectrum of the junction in the presence of an applied voltage: $G/G_N = \frac{1}{4}\sum_{\eta,\sigma}\int_{-\pi/2}^{\pi/2} d\theta\cos\theta(1 + |r_{\eta,\sigma}^h|^2 - |r_{\eta,\sigma}^e|^2)$. Note that an important difference from graphene is that here we cannot make use of a valley degeneracy: The contribution to the charge conductance from each valley must be computed separately. From the boundary conditions, one then obtains an explicit analytical expression for the normal and Andreev reflection coefficients as follows:

$$r_e = 2\cos\beta\Upsilon(\theta)\mathcal{D}^{-1},\quad r_h = 4e^{i(\eta\theta-\phi)}k_F\cos\theta\mathcal{D}^{-1}, \tag{4}$$

with $\Upsilon(\theta) = \sum_\pm \pm e^{\pm i\eta\theta}\tau_\mp$, $\mathcal{D} = 4(ik_F\sin\beta\cos\theta + E\cos\beta)$, and $e^{i\beta} = u_+/u_-$. As a consistency check, one may consider the "graphene" limit of the above results where $\lambda_{SO} = E_z = 0$. In this case, we have $k_F = \tau_\pm = E$, so that one finds $r_h = e^{-i(\beta+\phi)}$ for $\theta = 0$. This agrees with the result of Ref. [14], which found unity Andreev reflection probability even in the presence of a large Fermi vector mismatch (as in our case) for normal incidence. From the analytical expressions in Eq. (4), several observations can be made. First, the Andreev reflection process is independent of whether $E_z < E_c$ or $E_z > E_c$ as long as the deviation $|E_z - E_c|$ from the critical field is the same. This may be seen by noting that these two regimes are related via the substitutions $\tau_+ \leftrightarrow \tau_-$ for which $|r_h|^2$ and $|r_e|^2$ are invariant. Second, it is seen that the probability for Andreev reflection, and thus the conductance of the junction, may be altered considerably by tuning the applied electric field E_z. We illustrate this in Fig. 2, setting $\lambda_{SO}/\Delta_0 = 5$. For Figs. 2(a)–2(e), we consider the Andreev (solid lines) and normal (dashed lines) reflection probabilities as a function of bias voltage for normal incidence $\theta = 0$. Due

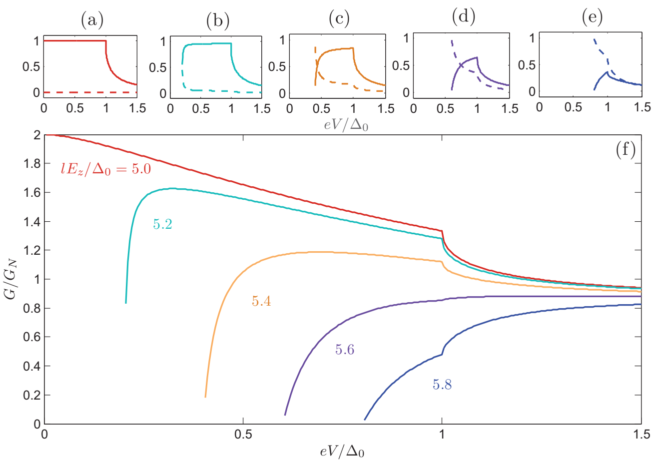

FIG. 2. (Color online) (a)–(e) Normal (dashed lines) and Andreev reflection (solid lines) probabilities for an N-S junction with $\eta = \sigma = +1$, $\lambda_{SO}/\Delta_0 = 5.0$, and lE_z/Δ_0 ranging from 5.0 to 5.8 from (a) to (e). In (f), the conductance G/G_N (averaged over spin and valleys) is plotted vs bias voltage for the same choices of lE_z/Δ_0.

to the band splitting in the N part, only the $\eta = \sigma = +1$ and $\eta = \sigma = -1$ bands contribute to transport, and we consider in Figs. 2(a)–2(e) the $\eta = \sigma = +1$ case without loss of generality for an applied electric field lE_z/Δ_0 ranging from 5.0 to 5.8. When the field is close to the critical one, E_c, the Andreev reflection probability totally dominates normal reflection and one finds that it is unity for subgap energies exactly when $E_z = E_c$. Upon increasing the field E_z and thus moving away from E_c, the normal reflection probability increases and eventually dominates Andreev reflection. Note that in each case, transport sets in only when eV exceeds the insulating gap, the latter varying in magnitude with E_z. The experimental signature of this tunable Andreev reflection is seen in the conductance G/G_N shown in Fig. 2(f): For fields close to E_c, the conductance is strongly enhanced at low bias voltages whereas it is suppressed at higher fields E_z where normal reflection dominates. In effect, the applied electric field controls the Andreev reflection process and correspondingly the conductance of the junction, enabling a switching from Cooper pair transport to normal-state scattering.

We now demonstrate that silicene offers a unique testbed for probing nonlocal transport in the form of crossed Andreev reflection. The experimental setup is shown in Fig. 1(d) and we assume as before a strongly doped superconducting region with large μ_S. The fact that both the insulating gap and the Fermi level in silicene (due to its low density of states) may be controlled simply by external electric fields or gate voltages [15] is the key to obtaining not only a *pure* CAR signal (without any elastic cotunneling) but also a nonlocal current which is *fully spin polarized* in each valley. To see how this may be obtained, let $2|m_{L,R}|$ denote the gap in the left and right normal silicene region between the lowest-lying conduction band and highest-lying valence band with $m = \lambda_{SO} - lE_z$. As in Fig. 1(b), the two other bands are assumed to be separated largely and thus do not contribute to transport. Setting the Fermi level to the top of the valence band in the right region ($\mu_R = -m_R$), the fate of nonlocal transport depends on the band structure in the left region. We consider here two scenarios: (i) There is no gap in the left region ($m_L = 0$) with $\mu_L = 0$, meaning that the electric field is equal to the critical value E_c, and (ii) there is a gap $2m_L$ in the left region and the Fermi level is tuned to lie right at the bottom of the conduction band ($\mu_L = m_L$). In case (i), Andreev reflection can occur in addition to normal reflection for any incident energy since there is no gap in the spectrum, whereas in the right region only CAR is possible. The reason is that an incident electron from the conduction band only has a gap to tunnel into in the right region. Consider now instead scenario (ii). In this case, local Andreev reflection is no longer possible since the spectrum is gapped on the left side. For the same reason as in case (i), elastic cotunneling is not possible either. This means that *only* normal reflection and CAR are physically allowed scattering processes for this system. We emphasize here that it is not crucial that the Fermi level lies exactly on the gap edge, as considered above: A deviation from this simply means that the current flow starts at a different applied voltage. We have chosen the above values to illustrate the principle used to obtain pure CAR as they offer the simplest visualization of the underlying idea.

The scattering probabilities are computed using the same method as in the N-S case, matching wave functions at the two interfaces with scattering coefficients r_e, r_h, t_h associated with normal reflection, Andreev reflection, and crossed Andreev reflection. It is important to note that the probability coefficients belonging for each process (R_e, R_h, T_h) must be derived from the continuity equation, and are not necessarily equal to simply the modulus square of the above quantities [11]. One obtains an expression for the (zero-temperature) nonlocal conductance G_{nl} which may be experimentally measured:

$$\frac{G_{nl}}{G_0} = \frac{1}{4}\sum_{\eta,\sigma}\int_{-\pi/2}^{\pi/2} d\theta \mathcal{P}_h |t_h|^2 \sqrt{q_F^h - k_y^2}, \qquad (5)$$

where $\mathcal{P}_h = 1/(E-\mu_R)$, $q_F^h = \sqrt{(\mu_R - E)^2 - m_R^2}$ is the wave vector of the CAR hole on the right side, $k_y = k_L \sin\theta$ is its transverse momentum, and G_0 is a normalization constant. To investigate quantitatively the probabilities for these reflection processes to occur, consider Fig. 3. We fix $\mu_S/\Delta_0 = 20$ and set the band gap to $m/\Delta_0 = 5$ when it is present in each region and also consider junction lengths $L \geqslant 2\xi$ where ξ is the superconducting coherence length, since the non-self-consistent approach used here is valid only for a sufficiently large superconducting region. In Fig. 3(a), the CAR process is shown both as a function of angle of incidence and junction length at a fixed voltage $eV/\Delta_0 = 0.9$ in the top panels and also as a function of bias voltage for a fixed junction length $L/\xi = 2.1$ for normal incidence in the bottom panels. As seen, both local and nonlocal Andreev reflections are possible in this case and the maximum probability reached for the CAR process is about 30% (we have verified this for other parameter choices). Still, it should be noted that CAR is the *only* nonlocal transport process available due to the Fermi level lying right at the top of the valence band, which means that the current in the right N part is carried solely by crossed Andreev reflected holes. This is in complete contrast to

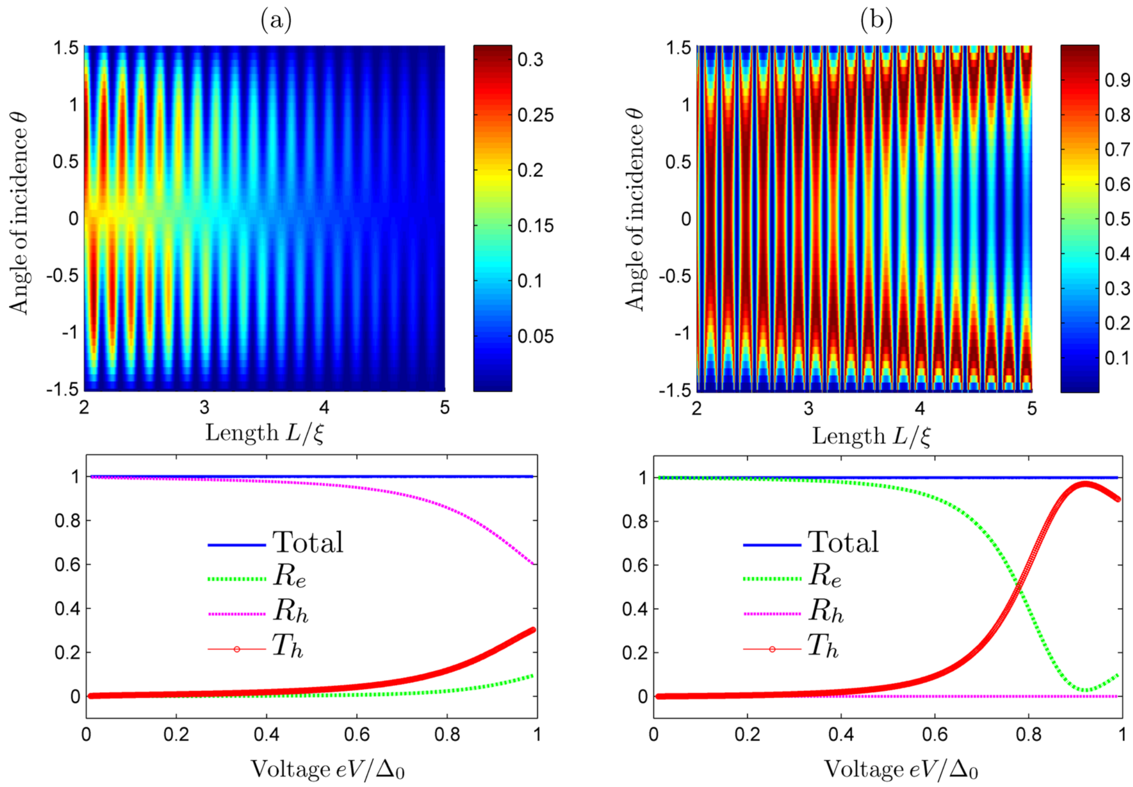

FIG. 3. (Color online) Top row: Contour plot of the CAR probability for a bias voltage $\mathrm{eV}/\Delta_0 = 0.9$ vs angle of incidence θ and junction length L. Bottom row: Probabilities for the different scattering events for a fixed junction length $L/\xi = 2.1$ for normal incidence. In column (a), we consider scenario (i) as described in the main text (nongapped-superconductor-gapped) whereas in (b) we consider scenario (ii) as described in the main text (gapped-superconductor-gapped). We have considered in all cases a strongly doped superconducting region with $\mu_S/\Delta_0 = 20$ and set $m_L/\Delta_0 = 0$ and $m_R/\Delta_0 = 5$ in (a) whereas $m_L/\Delta_0 = m_R/\Delta_0 = 5$ in (b). The coefficients (R_e, R_h, T_h) are the probabilities for normal, Andreev, and crossed Andreev reflection, respectively.

usual metallic systems which typically give the same order of magnitude for the probability of elastic cotunneling and CAR.

The situation becomes even more intriguing when considering scenario (ii), where now CAR is the only physically allowed process in addition to normal reflection. In this case, CAR probability reaches essentially 100%, meaning that *all* of the incoming electrons from the left N side combine with electrons from the right N side to produce Cooper pairs in the superconductor. A similar effect can be obtained at one specific voltage in graphene [16], but in that case elastic cotunneling occurs immediately upon deviating from that bias voltage. In the present case of silicene, there is no elastic cotunneling at all in the subgap regime and we have pure CAR at all voltages. In addition to generating a nonlocal Andreev (hole) current in this way, it is interesting to observe that this nonlocal current is fully spin-valley polarized, which has no counterpart in other semiconducting systems [17]. This means that in each valley, the current is fully spin polarized with opposite spin polarization in the two valleys such that the product spin $\otimes$ valley is conserved. The nonlocal conductance defined in Eq. (5) is shown in Fig. 4 and is seen to show similar behavior to that of the CAR probability.

Finally, we have also computed the supercurrent flow through silicene, by considering an S-N-S junction. This setup is experimentally viable and has previously been used to study the supercurrent through, e.g., graphene [18,19] and topological insulators [20–22]. We consider here ballistic transport which is appropriate under the assumption of relatively short junction lengths satisfying $L \ll \xi$. In such a scenario, the supercurrent is carried solely by Andreev bound states (ABS) existing in the junction. These bound states are formed by resonant Andreev reflections occurring at the two interfaces and may be computed by setting up similar wave functions as in the N-S case and identifying the resonance energies. We compute the spin- and valley-dependent ABS energies ε for a junction with a finite chemical potential μ_N in the normal region, which is assumed to cross both of the conduction bands. Denoting the superconducting phase difference as $\Delta\phi$ and setting $\mu_N \gg \Delta_0$, we find that

$$\frac{\epsilon(\Delta\phi)}{\Delta_0} = \pm\sqrt{\frac{4\mathcal{M}^2\cos^2(\Delta\phi/2) + L^2(\mathcal{M}^2 - k^2)^2}{4\mathcal{M}^2 + L^2(\mathcal{M}^2 - k^2)^2}} \qquad (6)$$

upon defining $\mathcal{M} = \mu_N + (\eta\sigma\lambda_{\mathrm{SO}} - lE_z)$ and $k = \sqrt{\mu_N^2 - (\eta\sigma\lambda_{\mathrm{SO}} - lE_z)^2}$. This gives rise to a supercurrent in the zero-temperature limit of the form

$$\frac{I(\Delta\phi)}{I_0} = \sum_{\eta\sigma} \frac{\mathcal{M}^2 \sin\Delta\phi}{[4\mathcal{M}^2 + L^2(\mathcal{M}^2 - k^2)^2]\epsilon(\Delta\phi)}. \qquad (7)$$

The most interesting aspect of the above equation is that it explicitly depends on the applied electric field E_z, suggesting

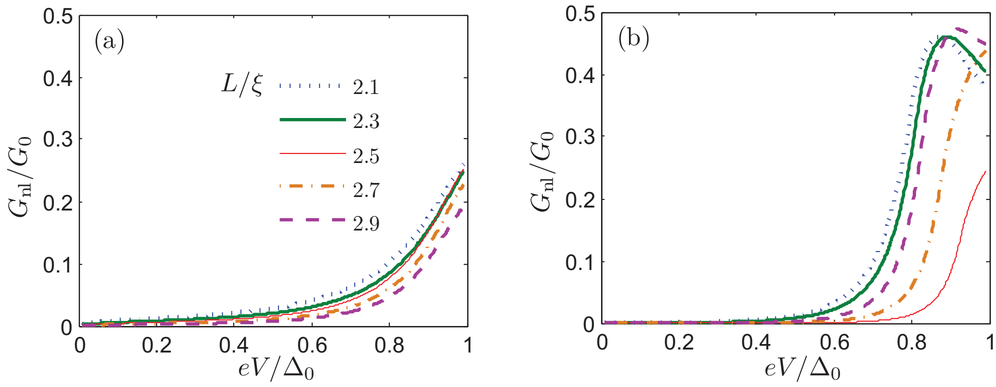

FIG. 4. (Color online) Nonlocal conductance for (a) gapless and (b) gapped silicene on the left side [corresponding to scenarios (i) and (ii) described in the main text].

that one may experimentally control the supercurrent in a given sample by tuning the field E_z. Moreover, in the case where the Fermi level only crosses the lowest conduction band ($\eta = \sigma = \pm 1$), the supercurrent is fully spin-valley polarized since Andreev reflection conserves this polarization.

To make a connection to the experimental arena, here we estimate the value required for some of the main parameters used in our calculations. The proximity-induced superconducting gap may be of order $\sim$1 meV according to experiments using a conventional s-wave superconductor contacted to a low-dimensional system with spin-orbit coupling (see, e.g., Ref. [23]). The spin-orbit coupling strength $\lambda_{\rm SO}$ has been computed to 3.9 meV by a first-principles calculation [13] which gives a critical electric field strength $E_c = 17$ meV/Å. It should be noted that very recent first-principles calculations [24] suggest that superconductivity could appear intrinsically in silicene [25] under specific conditions.

Looking forward, it would be interesting to investigate the effect of a magnetic exchange field [26] on our results to see, e.g., how it alters the spin-valley polarization of the supercurrent and if it is possible to obtain electrically controllable 0-π oscillations. We leave these issues for future investigations.

This work was supported by a Grant-in-Aid for Young Scientists (B) (No. 23740236) and the “Topological Quantum Phenomena” (No. 25103709) Grant-in Aid for Scientific Research on Innovative Areas from the Ministry of Education, Culture, Sports, Science and Technology (MEXT) of Japan and the COST Action MP-1201 “Novel Functionalities through Optimized Confinement of Condensate and Fields.”

[1] A. H. Castro Neto, F. Guinea, N. M. R. Peres, K. S. Novoselov, and A. K. Geim, Rev. Mod. Phys. **81**, 109 (2009).
[2] M. Z. Hasan and C. L. Kane, Rev. Mod. Phys. **82**, 3045 (2010).
[3] It is appropriate to mention here the Dirac fermions emerging in the low-energy sector of the pseudogap phase for high-$T_c d$-wave cuprates, which were discovered much earlier than either graphene or topological insulators.
[4] B. Lalmi, H. Oughaddou, H. Enriquez, A. Kara, S. Vizzini, B. Ealet, and B. Aufray, Appl. Phys. Lett. **97**, 223109 (2010); P. De Padova, C. Quaresima, C. Ottaviani, P. M. Sheverdyaeva, P. Moras, C. Carbone, D. Topwal, B. Olivieri, A. Kara, H. Oughaddou, B. Aufray, and G. Le Lay, *ibid.* **96**, 261905 (2010).
[5] K. Takeda and K. Shiraishi, Phys. Rev. B **50**, 14916 (1994).
[6] M. Ezawa, New J. Phys. **14**, 033003 (2012); Phys. Rev. Lett. **109**, 055502 (2012).
[7] X.-L. Qi and S.-C. Zhang, Rev. Mod. Phys. **83**, 1057 (2011).
[8] J. Alicea, Rep. Prog. Phys. **75**, 076501 (2012).
[9] C. W. J. Beenakker, Annu. Rev. Condens. Matter Phys. **4**, 113 (2013).
[10] M. Leijnse and K. Flensberg, Semicond. Sci. Technol. **27**, 124003 (2012).
[11] See Supplemental Material at http://link.aps.org/supplemental/10.1103/PhysRevB.89.020504 for additional details.
[12] C.-C. Liu, W. Feng, and Y. Yao, Phys. Rev. Lett. **107**, 076802 (2011).
[13] C.-C. Liu, H. Jiang, and Y. Yao, Phys. Rev. B **84**, 195430 (2011).
[14] C. W. J. Beenakker, Phys. Rev. Lett. **97**, 067007 (2006).
[15] In general, both E_z and μ can be influenced when altering the external field, although the exact details should depend on the experimental setup, such as the substrate.
[16] J. Cayssol, Phys. Rev. Lett. **100**, 147001 (2008).
[17] M. Veldhorst and A. Brinkman, Phys. Rev. Lett. **105**, 107002 (2010).
[18] M. Titov and C. W. J. Beenakker, Phys. Rev. B **74**, 041401 (2006).
[19] J. Linder, T. Yokoyama, D. Huertas-Hernando, and A. Sudbo, Phys. Rev. Lett. **100**, 187004 (2008).
[20] L. Fu and C. L. Kane, Phys. Rev. B **79**, 161408(R) (2009).
[21] Y. Tanaka, T. Yokoyama, and N. Nagaosa, Phys. Rev. Lett. **103**, 107002 (2009).
[22] J. Linder, Y. Tanaka, T. Yokoyama, A. Sudbo, and N. Nagaosa, Phys. Rev. B **81**, 184525 (2010).
[23] M.-X. Wang, C. Liu, J.-P. Xu, F. Yang, L. Miao, M.-Y. Yao, C. L. Gao, C. Shen, X. Ma, X. Chen, Z.-A. Xu, Y. Liu, S.-C. Zhang, D. Qian, J.-F. Jia, and Q.-K. Xue, Science **336**, 52 (2012).
[24] W. Wan, Y. Ge, F. Yang, and Y. Yao, Europhys. Lett. **104**, 36001 (2013).
[25] L. Chen, B. Feng, and K. H. Wu, Appl. Phys. Lett. **102**, 081602 (2013).
[26] T. Yokoyama, Phys. Rev. B **87**, 241409(R) (2013).